A Novel Valence-Bond-Based Automatic Diabatization Method by Compression

Yang Zhang, Peifeng Su, Benjamin Lasorne, Benoît Braïda, Wei Wu

A Novel Valence Bond based Automatic Diabatisation Method by Compression

Yang Zhang,[1] Peifeng Su,[1*] Benjamin Lasorne,[2*] Benoît Braïda,[3] Wei Wu[1]

[1]*Fujian Provincial Key Laboratory of Theoretical and Computational Chemistry, The State Key Laboratory of Physical Chemistry of Solid Surfaces, and College of Chemistry and Chemical Engineering, Xiamen University, Xiamen, Fujian 361005, China*

[2]*ICGM, Univ Montpellier, CNRS, ENSCM, Montpellier, France*

[3]*Laboratoire de Chimie Théorique, Sorbonne Université, CNRS, Paris, France*

Abstract A novel valence bond based automatic diabatisation method by compression, called valence bond based compression approach for dibatization (VBCAD), is presented in this letter. It is a "black-box" type method that provides an automatic diabatisation from a classical valence bond (VB) perspective. In VBCAD, a model space projection is performed by an eigenvalue decomposition algorithm followed by dimensional reduction based on a sequence of Householder transformations. Our diabaticity criterion is implemented in a way that maximizes the diversity of VB structure weights between different diabatic states. Owing to the rigorous Householder transformations employed in this entire procedure, the invariance of the target eigensubspace is preserved. This is illustrated on two prototypical examples.

[*] To whom correspondence should be addressed.

Table of Content (TOC)

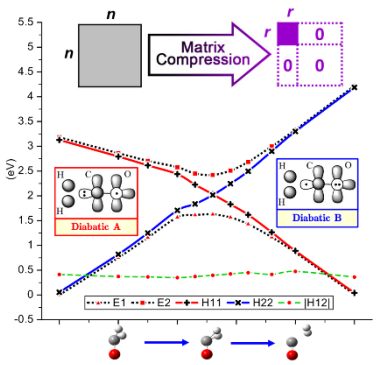

It is well established that the Born-Oppenheimer (B.O.) approximation breaks down near conical intersections or avoided crossings, where at least two adiabatic states are degenerate or nearly degenerate. As a consequence, the molecular Hamiltonian must account for non-adiabatic coupling terms (NACT) among more than one adiabatic states, which still represents a challenge for its implementation within quantum dynamics simulations. The typical procedure relies on a unitary change of electronic basis, the so-called diabatic states, which are defined so as to reduce the magnitude of NACTs and make them negligible in molecular Hamiltonians. As such, the singular kinetic NACT vectors can be replaced by coupled potential energy surfaces that are smoothly varying functions of the nuclear coordinates. In principle, the construction of approximate diabatic states is not unique. The direct way that stems from their formal definition requires the determination of all derivative couplings over an extended range of nuclear coordinates, which involves large computational efforts[1-4]. Therefore, some alternative strategies have been proposed over the years, based on the properties of the adiabatic wave functions, whereby the adiabatic-to-diabatic (ATD) transformation is defined in order to enforce the smoothness of physical properties[5-9], or of the expressions of the electronic wave functions in terms of configurations[10-16]. As large non-adiabatic couplings are related to fast changes of the adiabatic wave functions with respect to the nuclear coordinates, the key of these strategies is to construct the ATD transformation from its ability to reduce the changes. In particular, the diabatic states can be obtained from the concept of block-diagonalization of the Hamiltonian[17-19], which can be derived from a least action principle.

In classical VB theory, the wave function of a many-electron system can be generally expressed as a linear combination of VB structures[20],

$$\Psi = \sum_K C_K \Phi_K \tag{1}$$

where C_K is the coefficient of VB structure Φ_K. In classical VB theory, the VB structures are constructed by using VB orbitals that are strictly localized on an atom or fragment. To do so, each VB orbital is defined as a linear combination of a subset of the basis functions, including the basis functions

centered only on a chosen atom or fragment. Among various classical VB methods, VBSCF, which optimizes structure coefficients and orbitals simultaneously, is the basic method of *ab initio* classical VB theory. Each VB structure is defined by a particular configuration of electrons (understood as a given occupancy of the VB orbital set) together with a specific spin function. As such, each VB structure corresponds to a particular bonding scheme that is kept invariant irrespective of the variations of molecular geometries, and, can be mapped to a specific Lewis structure. Therefore, classical VB theory appears as a natural choice from a chemical perspective in the construction of diabatic states. Recently, *ab initio* classical VB methods and block-localized wave function (BLW), which is a type of semi-localized VB method that uses a single-determinantal wave function built on semi-localized molecular orbitals, have been successfully employed in the direct construction of diabatic states, based on the assumption that an educated inspection of dominant VB structure sets can be associated with the diabatic states[21-23].

In this letter, we go beyond this assumption and present a novel method named valence bond based compression approach for dibatization (VBCAD). In the VBCAD scheme, diabatic states are obtained by a sequence of rigorous unitary transformations that keeps the invariance of the target eigensubspace. The whole procedure is schematically presented in the flowchart displayed in Figure 1. The central idea of VBCAD is to employ first a projection to reduce the full Hamiltonian to a low rank matrix that preserves the target eigensubspace. This is followed by a sequence of Householder transformations (prediagonalisation) coupled to a VB based diabatisation criterion that produces the diabatic low rank and low dimension block of interest. The whole procedure ensures smoothness of the final diabatic matrix elements with respect to variations in the nuclear coordinates (molecular geometry). The different steps of the VBCAD procedure are detailed in the following.

(Figure 1. near here)

In order to facilitate the following eigenvalue decomposition (ED) formalism with the non-orthogonal

VB structure set, which is used in VBSCF calculation, it is convenient but not unique to start with a symmetric Löwdin orthogonalization[24-25], i.e.:

$$\mathbf{H}^{\mathrm{L}} = (\mathbf{M}^{-\frac{1}{2}})^{\mathrm{T}}\,\mathbf{H}(\mathbf{M}^{-\frac{1}{2}}) \tag{2}$$

where **H** and **M** are the VB Hamiltonian and overlap matrices, respectively.

The rank reduction trick starts from ED, which is a factorization of the form,

$$\mathbf{H}^{\mathrm{L}} = \mathbf{Q}\boldsymbol{\Sigma}\mathbf{Q}^{-1} \tag{3}$$

where: i) **Q** is an orthogonal matrix ($\mathbf{Q}\mathbf{Q}^{\mathrm{T}}=\mathbf{I}$) made of the VB structure coefficients for each adiabatic state wave function ; and: ii) $\boldsymbol{\Sigma}$ is a square diagonal matrix with the eigenvalues $\varepsilon_1, ..., \varepsilon_n$, where n is the number of VB structures.

$\mathbf{H}^{\mathrm{L}}$ can be expanded into two matrices by the relation:

$$\mathbf{H}^{\mathrm{L}} = \mathbf{Q}\begin{pmatrix} \boldsymbol{\Sigma}_{\mathrm{e}} & \mathbf{0} \\ \mathbf{0} & \mathbf{0} \end{pmatrix}\mathbf{Q}^{-1} + \mathbf{Q}\begin{pmatrix} \mathbf{0} & \mathbf{0} \\ \mathbf{0} & \boldsymbol{\Sigma}_{\mathrm{n}} \end{pmatrix}\mathbf{Q}^{-1} = \mathbf{H}^{\mathrm{e}} + \mathbf{H}^{\mathrm{n}} \tag{4}$$

where $\boldsymbol{\Sigma}_{\mathrm{e}}$ and $\boldsymbol{\Sigma}_{\mathrm{n}}$ denote the diagonal matrices with eigenvalues ε_1, ..., ε_r and ε_{r+1}, ..., ε_n respectively, with r the number of electronic states that are required to describe the system under study over a representative range of nuclear coordinates (i.e.: r is the dimension of the target space). The feature of the projected ED approach is that the model subspace is isolated. This means that the following matrix compression will be performed on $\mathbf{H}^{\mathrm{e}}$ with reduced rank r rather than on $\mathbf{H}^{\mathrm{L}}$ with full rank n.

A series of Householder matrices are then used to achieve the dimensional reduction in the proposed method. In this sense, the symmetric high dimension ($n\times n$) matrix $\mathbf{H}^{\mathrm{e}}$ can be reduced into a low dimension ($r\times r$) matrix $\mathbf{H}^{\text{pre-dia}}$, which is termed “pre-diabatic”:

$$\mathbf{H}^{\text{pre-dia}} = \mathbf{P}^{-1}\mathbf{H}^{\mathrm{e}}\mathbf{P} \tag{5}$$

$\mathbf{H}^{\text{pre-dia}}$ is obtained by the following recursion formula:

$$\mathbf{H}_{i+1}^{e} = \mathbf{P}_i \mathbf{H}_i^{e} \mathbf{P}_i \quad (i=1, 2, \ldots, n\text{-}1) \tag{6}$$

in which the i^{th} transformation $\mathbf{P}_i$ is defined as:

$$\mathbf{P}_i = \mathbf{I} - 2\omega_i \omega_i^{T} \tag{7}$$

where ω_i is a column unit vector related to the matrix elements in $\mathbf{H}_i^{e}$. The detailed definition of ω_i is provided in **Appendix.**

Sequentially, the VB structure coefficients of pre-diabatic wave functions are obtained by the relations:

$$\mathbf{C}^{\text{pre-dia}} = \mathbf{M}^{-\frac{1}{2}} \mathbf{P} \mathbf{C}^{e} \tag{8}$$

where $\mathbf{C}^{e}$ is a coefficient matrix of dimension ($n \times r$) with the eigenvector of $\mathbf{\Sigma}_e$ on each column respectively, and $\mathbf{M}^{-\frac{1}{2}}$ comes from the symmetric Löwdin orthogonalization. It should be noticed here that this Householder reduction algorithm is feasible for any number of states of interest.

The final transformation from the pre-diabatic Hamiltonian to the diabatic Hamiltonian is achieved by the following unitary transformation:

$$\mathbf{U}^{-1} \mathbf{H}^{\text{pre-dia}} \mathbf{U} = \mathbf{H}^{\text{dia}} \tag{9}$$

For the special case r=2, the unitary matrix **U** can be defined as a two-step Householder transformation with two variables, by the relation:

$$\mathbf{U}(\alpha, \beta) = \mathbf{U}_1(\alpha) \mathbf{U}_2(\beta) \tag{10}$$

where $\mathbf{U_1}(\alpha)$ and $\mathbf{U_2}(\beta)$ are Householder matrices defined by **eq.7**, in which

$$\omega_1 = (\sin\alpha, \cos\alpha, 0, \ldots, 0)^{T}; \ \omega_2 = (\sin\beta, \cos\beta, 0, \ldots, 0)^{T} \tag{11}$$

Now the key point becomes how to characterize the diabatic states. This means that a specific diabaticity criterion is required so as to act as a constraint to make **eq.9** nonarbitrary. Taking advantage of the characteristics of classical VB structures, principally their direct and unchanged connection with

specific Lewis structures, we propose here a novel approach, whereby the diabaticity criterion is chosen as a quantity that maximizes the separation of VB structure weights in different states. This criterion was implemented in VBCAD to obtain the diabatic states in such a way that, in **eq.9**, $\mathbf{U}(\alpha,\beta)$ is determined by maximizing the quantity $F[\mathbf{U}(\alpha,\beta)]$ defined as:

$$F[\mathbf{U}(\alpha,\beta)] = \sum_{K}^{n} \left| W_{K,1}(\alpha,\beta) - W_{K,2}(\alpha,\beta) \right| \tag{12}$$

where n is the number of VB structure, 1 and 2 correspond to the two diabatic states, $W_{K,i}$ is the weight of structure K in the diabatic state i. Among various available definitions of structure weights, the simplest renormalized definition of VB weights was employed here. Within this definition, the VB structure weights W_K are obtained as:

$$W_K = NC_K^2; N = \sum_{K}^{n} \frac{1}{C_K^2} \tag{13}$$

where C_K is the coefficient of structure K in a given diabatic state.

This particular choice of $\mathbf{U}(\alpha,\beta)$ will be referred to as $\mathbf{U}(\alpha,\beta)_{\max}$ in the following. Therefore, the diabatic Hamiltonian $\mathbf{H}^{\text{dia}}$ is obtained from **eq.9**:

$$\mathbf{U}^{-1}(\alpha,\beta)_{\max} \mathbf{H}^{\text{pre-dia}} \mathbf{U}(\alpha,\beta)_{\max} = \mathbf{H}^{\text{dia}} \tag{14}$$

The VB coefficients of both diabatic states, which are denoted as $\mathbf{C}^{\text{dia}}$, are obtained from:

$$\mathbf{C}^{\text{dia}} = \mathbf{U}(\alpha,\beta)_{\max} \mathbf{C}^{\text{pre-dia}} \tag{15}$$

Subsequently, the attribution of pointwise diabatic states can be determined according to the minimum change in coefficients.

Two examples, the torsion of ethylene (C_2H_4) and the photo-dissociation of formaldehyde (H_2CO), are presented to illustrate our method. For the torsion of ethylene the adiabatic states were calculated by the VBSCF method with six active electrons in six active orbitals. The strictly-localized valence orbitals were recombined in symmetry-adapted semi-localized orbitals to match the symmetry of the

D_2 point group at all twisted geometries. The dihedral angle ∠H-C-C-H was varied from 0° to 180°, while the bond lengths of the four C-H bonds and C-C bond were fixed at 1.070 Å and 1.355 Å respectively. The energies of the lowest two adiabatic states of A symmetry together with the diabatic energy curves obtained through the VBCAD procedure are presented in **Figure. 2**.

(Figure 2. near here)

Note that the first A state is the ground state (N state), while the second A state is essentially the doubly excited state for the ππ* system (Z state). As expected, our results show that the two corresponding adiabatic energies exhibit an avoided crossing around the perpendicular geometry, while the character of the two states switches along the pathway. This is reflected by the crossing of the H_{11} and H_{22} curves. The two diabatic states thus transform smoothly with the variation of the dihedral angle. Furthermore, the VBCAD scheme deals correctly with the region of the avoided crossing, in the middle of the reaction path. This means that the numerical values of H_{12}, which have the meaning of a "diabatic coupling", vary little with respect to the central value that can be calculated directly when $H_{11} = H_{22}$,

$$H_{12} = \frac{1}{2}\left(E_2 - E_1\right) \tag{16}$$

where E_1 and E_2 are the energies of the adiabatic states. Further from the avoided crossing region the diabatic coupling term, H_{12}, varies smoothly and decays to nearly zero at the planar geometries.

In order to estimate the variance between pre-diabatic and diabatic states, the overlaps of the wave functions, $\left\langle \Psi^{\text{pre-dia}} \middle| \Psi^{\text{dia}} \right\rangle$, are computed pointwise, as shown in **Figure 3**. It comes out that the average values of the overlaps are close to 1 along the pathway, which means that the "pre-diabatic" states are already good approximations of the diabatic states that were obtained by further maximizing the difference of composition of the wave functions in terms of VB structures.

(Figure 3. near here)

Let us now move to our second numerical example. The photoexcitation of formaldehyde can

lead either to the loss of H_2 (molecular dissociation), or to the loss of H (radical dissociation) [26]. The non-adiabatic reaction path for the H_2 + CO molecular dissociation along a C_S symmetry-preserving pathway is explored here. The six electronic states that should be considered in a complete treatment of this dissociation pathway are displayed in **Figure 3**, and will be referred to as S_0-S_6 in the following. As can be seen on the figure, an avoided crossing occurs between the S_0 and S_2 states of A' symmetry, which will be a particularly interesting region to test the efficiency of our VBCAD methodology.

An accurate treatment of this dissociation pathway requires an active space of eight electrons into seven active orbitals, leading to a set of 490 VB structures on which the different states expand (eq 1). The full VBSCF adiabatic energy curves of the six states are shown in **Figure 4**. From the adiabatic curves we can see that two adiabatic states exhibit an S_0/S_2 avoided crossing along the reaction coordinate around point 10. It should be noted here that around the dissociation region, the excited states are highly degenerate and a more detailed analysis of them is beyond the scope of this paper. As a consequence, the region around the S_0/S_2 avoided crossing (from point 9 to point 12 in **Figure 4.**) can be simplified as a two-state case. The results are presented in **Figure 5.** The absolute value of the off-diagonal element does not vary much as a function of the reaction coordinate. This is indicative of the diabatic character of the representation produced by VBCAD. As can be seen from **Figures 6** (a) and (b), in contrast with the sudden change in the electronic nature of the adiabatic states, the diabatic states preserve their respective natures and are mainly governed by VB structure groups with specific electron occupation: one (green curve) is dominated by a group of VB structures with a doubly-occupied lone-pair on the O atom with a single electron on C(σ), while the other (red curve) is dominated by that of a singly-occupied lone-pair on the O atom with two electrons on C(σ). The analysis from **Figure 6** (c) suggests a possible electron transfer between the O and C atoms around the avoided crossing region. Such information on the chemical nature of the diabatic states was obtained automatically through VBCAD but was not so obvious *a priori* from a simple inspection of VB structures. This illustrates the capabilities of our approach in situations where diabatic states are not

obvious from the onset.

(Figures.4, 5 and 6 near here)

In order to further verify the diabaticity of states obtained by VBCAD, the residual non-adiabatic coupling (RNAC) is evaluated numerically. The RNAC is expressed as:

$$\left\langle \Psi_\alpha;\mathbf{Q}\middle|\Psi_\beta;\mathbf{Q}+\delta\mathbf{Q}\right\rangle \approx \left\langle \Psi_\alpha;\mathbf{Q}\middle|\Psi_\beta;\mathbf{Q}\right\rangle + \sum_K \left\langle \Psi_\alpha;\mathbf{Q}\middle|\frac{\partial\Psi_\beta}{\partial Q^K};\mathbf{Q}\right\rangle \delta Q^K = \delta_{\alpha\beta} + \sum_K D^K_{\alpha\beta}(\mathbf{Q})\delta Q^K \quad (17)$$

where α and β are the labels of the two states, $\mathbf{Q}$ is the set of nuclear coordinates, K is the index of the degree of freedom. For the states to be (quasi) diabatic, the non-adiabatic coupling must satisfy the following criterion:

$$D^K_{\alpha\beta}(Q) \approx 0 \quad (18)$$

Thus, evaluating the overlap between the two states along a pathway will give a measure of diabaticity: it has to be near $\delta_{\alpha\beta}$ for the non-adiabatic coupling to be small. Since the diabaticity of each VB structure is maintained by the electron-pairing pattern, and it varies little with the variation of the nuclear coordinates, the overlap between the two states along a pathway can be approximately obtained by the "dot product" of VB structure coefficients of the two states, which becomes a feasible way to evaluate the RNAC. The numerical results are shown in **Table.1**, which suggest that the values of RNAC are small, as expected for genuine diabatic states.

(Table.1 near here)

In summary, a novel valence bond based automatic diabatisation method by compression, referred to as VBCAD, is presented. It allows a low-dimensional effective Hamiltonian to be built, based on a diabatic VB expansion. VBCAD is "black-box" with no parameter involved in the whole procedure.

This is also a pointwise method which thus can be turned into a global diabatisation technique without line-integration along a path. In VBCAD, the model space projection is implemented by an eigenvalue decomposition (ED) algorithm followed by a sequence of Householder compressions, then the diabaticity criterion that makes use of maximally separated VB character is imposed through a final Householder transformation step. This diabatisation procedure keeps the invariance of the subspace spanned by each eigenstate of interest during the compression. It is appealing that the automation in VBCAD strategy provides a practical way of automatic inspection of VB structures based on the contributions of each diabatic state. The examples shown here illustrate that there is a real possibility for *ab initio* VB calculations to achieve the production of diabatic states by Householder matrix compression. Finally, it should be noted that we did not consider dynamic correlation here. VBSCF calculations for strongly correlated systems may not be accurate enough, and can be improved by using post-VBSCF methods[27-31]. This will be considered and developed in the future, as well as the generalization of the algorithm used for VBCAD to cases with more than two states.

The computational details are summarized as follows: The full Hamiltonian and overlap matrices were calculated with the Xiamen Valence Bond (XMVB) program[32]. The reaction path of formaldehyde was obtained with the GAUSSIAN16 software[33]. The basis set 6-31G* was used in all calculations. The diabatisation procedure was performed by a post-processing algorithm with the MATLAB program version 2018b[34].

Appendix

Here we introduce the Householder compression in a detailed way. In the main body of the paper, we focus on a special case with r=2 as an illustration, in which the *Householder tri-diagonalization*[35] and *Householder compressor*[36] algorithms are well suited for the proposed method.

For the 1st to (n-2)th step of transformation in **eq.5**,

$$\omega_i = [a_{i,1};\, a_{i,2};\ldots;\, a_{i,n-i};\, 0;\, \ldots;\, 0]^{\mathrm{T}} \tag{A-1}$$

$$\omega_i^{\mathrm{T}}\omega_i = 1 \tag{A-2}$$

where ω_i is a column vector related to the matrix elements in $\mathbf{H}_i^{\mathrm{e}}$, with the non-zero coefficients $a_{i,k}$ defined in the following. Because the transformation with $\mathbf{P}_i$ (eq.6) leaves the last (i-1) row and column unaltered, hence the last several elements of ω_i are chosen to be zero.

First, σ_i and G_i are defined by,

$$\sigma_i = \left(H^{\mathrm{e}}_{n-i+1,1}\right)^2 + \left(H^{\mathrm{e}}_{n-i+1,2}\right)^2 + \cdots + \left(H^{\mathrm{e}}_{n-i+1,n-i}\right)^2 \tag{A-3}$$

$$G_i = \sigma_i + H^{e}_{n-i+1,n-i}\sqrt{\sigma_i} \tag{A-4}$$

Then ω_i is obtained with each of the non-zero element computed by the relations,

$$a_{i,j} = \frac{H^{e}_{n-i+1,j}}{\sqrt{2G_i}};\left(j = 1,2,\cdots,n-i-1\right) \tag{A-5}$$

$$a_{i,n-i} = \frac{H^{e}_{n-i+1,n-i} + \sqrt{\sigma_i}}{\sqrt{2G_i}} \tag{A-6}$$

After the Householder tri-diagonalization, the $\mathbf{H}^{\mathrm{e}}$ with rank r can be reduced to a $(r+1)\times(r+1)$ tridiagonal matrix. In the next step, it can be further transformed perfectly into a smaller $r\times r$ full rank submatrix by means of a two-side Householder compressor $\mathbf{P}_{\mathrm{n-1}}$. Here we define $\boldsymbol{u}$ as a column vector corresponding to the one-dimensional null-space after tri-diagonalization of $\mathbf{H}^{\mathrm{e}}$, u_{i} is the i-th element, expressed by

$$u = \left(u_1, u_2, \cdots, u_{r+1}, 0, \cdots, 0\right)^{\mathrm{T}} \tag{A-7}$$

The $(n\text{-}1)^{\text{th}}$ transformation in **eq.6** defined by **eq.7** acts as a compressor, in which $\omega_{n\text{-}1}$ is computed by the relations,

$$\omega_{n-1} = \left(\frac{u_1}{-\sqrt{2-2u_{r+1}}}, \cdots, \frac{u_r}{-\sqrt{2-2u_{r+1}}}, \sqrt{\frac{1-u_{r+1}}{2}}, 0, \cdots, 0 \right)^{\mathrm{T}} \tag{A-8}$$

With these choices of n-1 Householder matrices above, $\mathbf{H}^{\mathbf{e}}$ becomes a full-rank matrix $\mathbf{H}^{\text{pre-dia}}$ with *rank r*.

Acknowledgement:

This project is supported by the National Natural Science Foundation of China (No. 21733008), New Century Excellent Talents in Fujian Province University and the Fundamental Research Funds for the Central Universities (No. 20720190046).

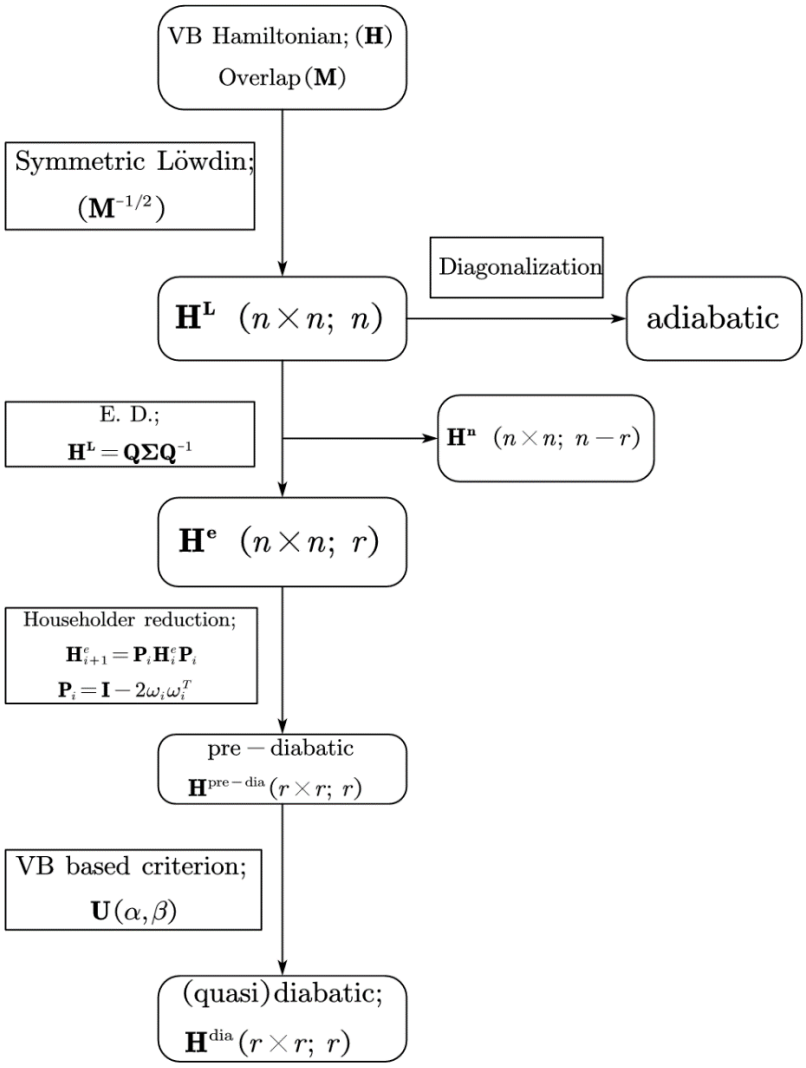

Figure 1. Flowchart representing the different steps of the VBCAD framework, with *n* the full dimensionality of the problem into study, and *r* the dimensionality of the reduced target space.

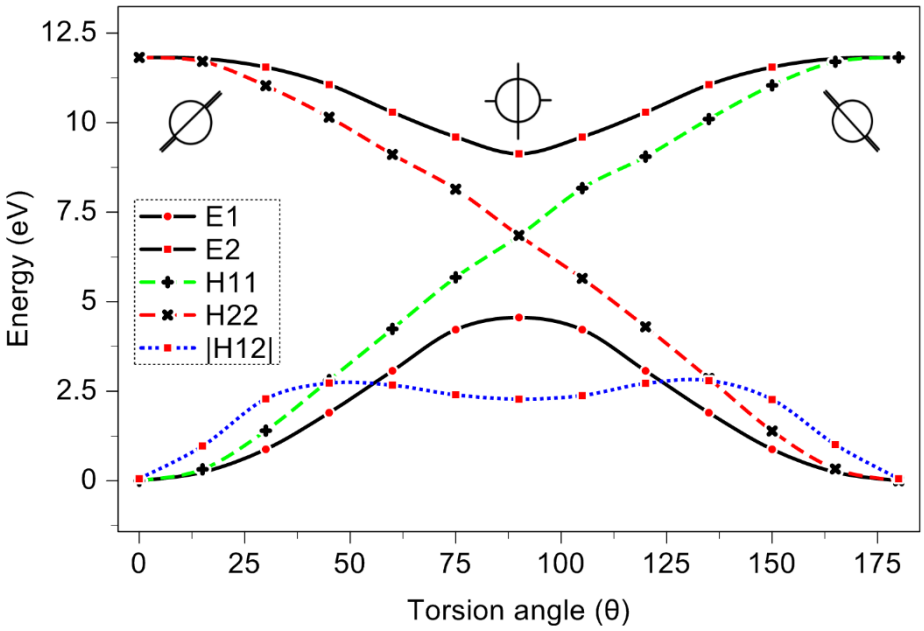

Figure 2. Black continuous curves: energy evolution (E1 and E2) of the lowest two *adiabatic A* states of C_2H_4 along the torsion coordinate describing a D_2-symmetry preserving pathway; red and green dashed lines: the diagonal diabatic energies H_{11} and H_{22} as obtained through the VBCAD procedure; blue dotted line: the diabatic coupling term H_{12}.

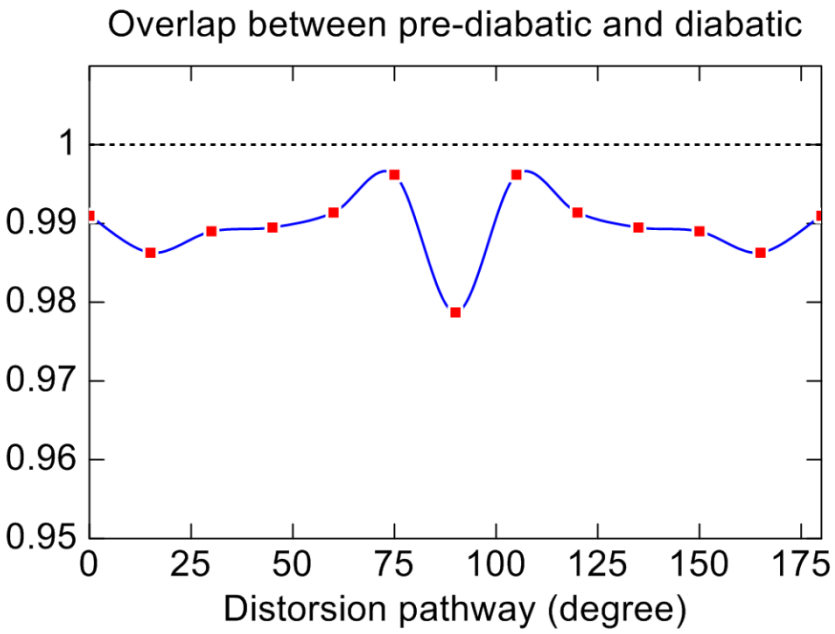

Figure 3. Wave function overlap between pre-diabatic and diabatic states along the distortion pathway.

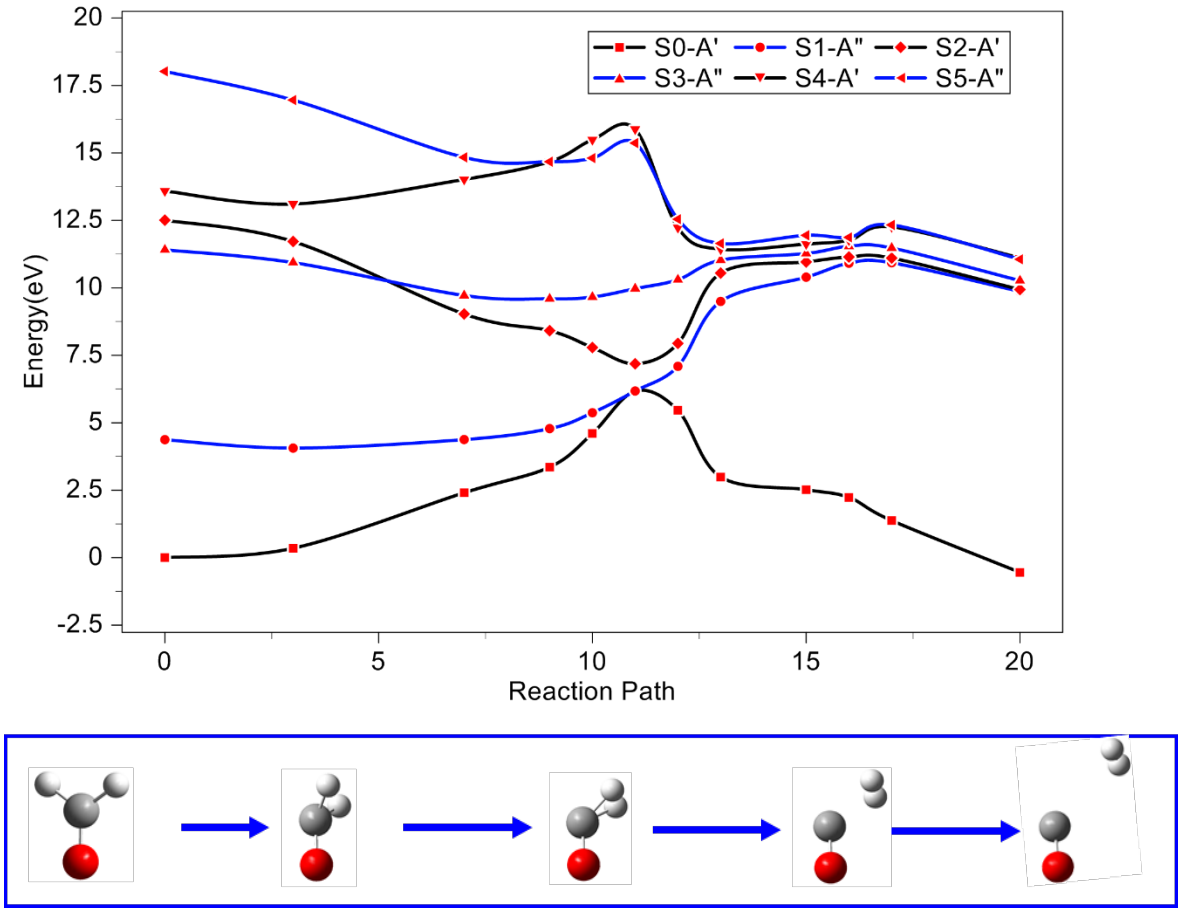

Figure 4. Energy curves for the photodissociation of formaldehyde along a C_s pathway. Black lines correspond to the three lowest lying A' states, blue lines to the three lowest lying A" states.

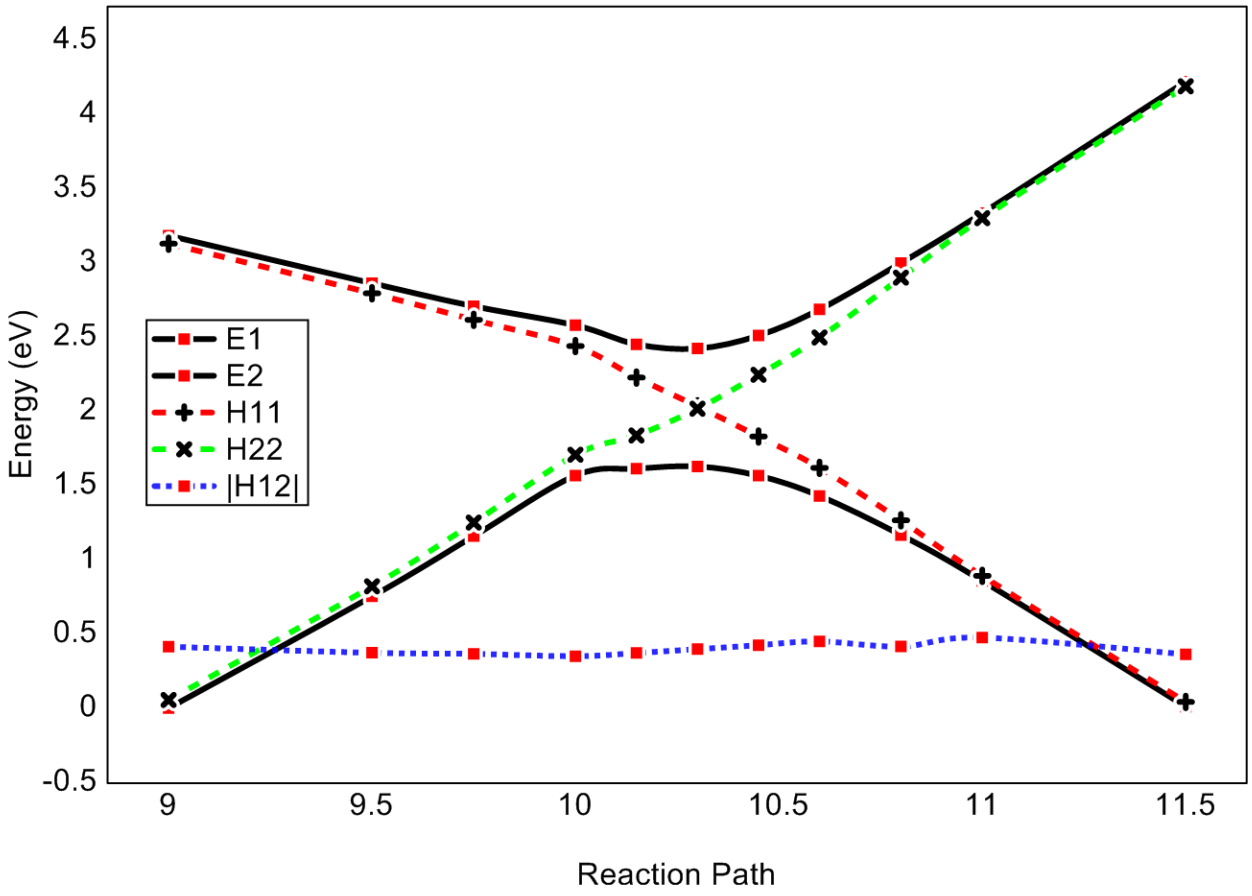

Figure 5. VBCAD results for the photodissociation of formaldehyde along a C_s pathway around the avoided crossing region. The black lines correspond to the two lowest lying A' adiabatic states. Green and red dashed lines represent the diabatic energy curves (diagonal terms of the Hamiltonian), and the blue dotted line the coupling term (off-diagonal term of the Hamiltonian) between them. The zero point is the S0 state at point 9, corresponding to the value 3.36 eV in Figure 4.

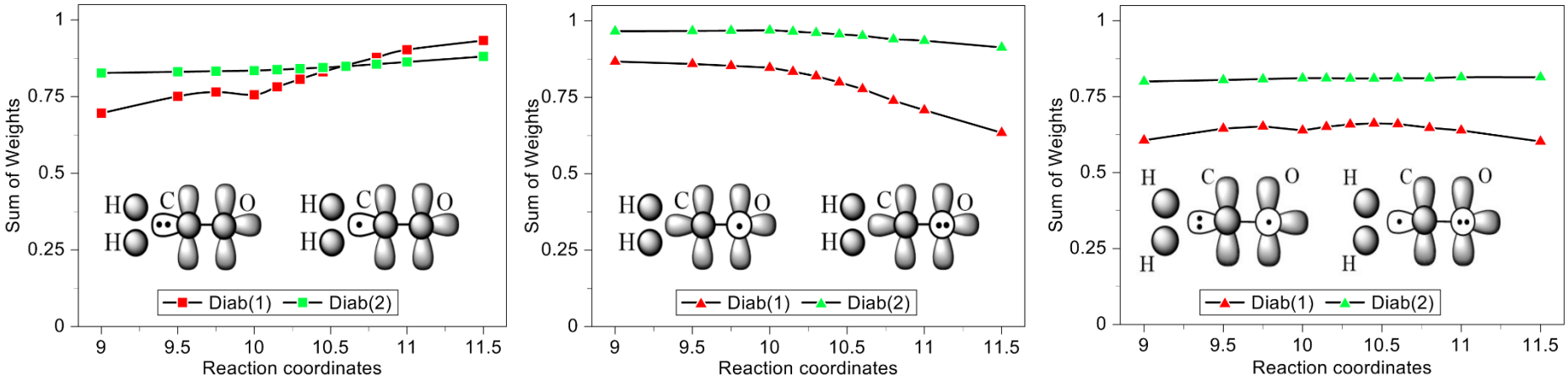

Figure 6. The specific VB structure group weights of two diabatic states around the avoided crossing region. The curve with red and green dots denotes the H_{11} and H_{22} diabatic states respectively. Y-axis displays the sum of weights of VB structures that describe the electron occupation on: (*a*) C(σ) orbital; (*b*) O(n) orbital; (*c*) both C(σ) orbital and O(n) orbital.

$\left\langle \Psi^{\text{dia}};R_x \middle\vert \Psi^{\text{dia}};R_y \right\rangle$	**<9|9.5>**	**<9.5|10>**	**<10|10.5>**	**<10.5|11>**	**<11|11.5>**
Diab_a	0.9940	0.9951	0.9754	0.9548	0.9762
Diab_b	0.9989	0.9982	0.9970	0.9947	0.9958

Table 1. The $\left\langle \Psi_1^{\text{dia}};R_x \middle\vert \Psi_2^{\text{dia}};R_y \right\rangle$ values for the two diabatic states; R_x and R_y denote successive points along the reaction coordinate.

REFRENCE

(1) Smith, T. F. Diabatic and Adiabatic Representations for Atomic Collision Problems. *Phys. Rev.* **1969**, *179*, 111-123.

(2) Baer, M. Adiabatic and Diabatic Representations for Atom-Molecule Collisions: Treatment of the Collinear Arrangement. *J Chem. Phys. Lett.* **1975**, *35*, 112-118.

(3) Top, Z. H.; Baer, M. Incorporation of Electronically Nonadiabatic Effects into Bimolecular Reactive Systems. I. Theory. *J. Chem. Phys.* **1977**, *66*, 1363.

(4) Baer, M. Electronic Non-Adiabatic Transitions Derivation of the General Adiabatic-Diabatic Transformation Matrix. *Mol. Phys.* **1980**, *40*, 1011-1013.

(5) Mulliken, S, R. Molecular Compounds and Their Spectra. II . *J. Am. Chem. Soc.* **1952**, *74*, 811-824.

(6) Werner, H. J.; Meyer, W. MCSCF Study of the Avoided Curve Crossing of the Two Lowest1σ+States of LiF. *J. Chem. Phys.* **1981**, *74*, 5802-5807.

(7) Hush, N. S. Intervalence-Transfer Absorption. II . Theoretical Considerations and Spectroscopic Data; *Progress in Inorganic Chemistry* **1967,** *391-444*.

(8) Cave, R. J.; Newton, M. D. Calculation of Electronic Coupling Matrix Elements for Ground and Excited State Electron Transfer Reactions: Comparison of the Generalized Mulliken–Hush and Block Diagonalization Methods. *J. Chem. Phys.* **1997**, *106*, 9213-9226.

(9) Ren, M.; Ma, B.; Chen, Z.; Wu, W. Two-Dimensional Analysis of the Diabatic Transition of a General Vectorial Physical Observable Based on Adiabatic-to-Diabatic Transformation. *J. Phys. Chem. Lett.* **2019**, *10*, 5868-5872.

(10) Hendekovic, Josip. Novel Variational Definition of Diabatic States. *Chem. Phys. Lett.* **1982**, *90*, 193-197.

(11) Ruedenberg, K.; Atchity, G. J. A Quantum Chemical Determination of Diabatic States. *J. Chem. Phys.* **1993**, *99*, 3799-3803.

(12) Atchity, G. J.; Ruedenberg, K. Determination of Diabatic States through Enforcement of Configurational Uniformity. *Theor. Chem. Acc.* **1997**, *97*, 47-58.

(13) Nakamura, H.; Truhlar, D. G. The Direct Calculation of Diabatic States Based on Configurational Uniformity. *J. Chem. Phys.* **2001**, *115*, 10353-10372.

(14) Spiegelmann, F.; Malrieu, J. P. The Use of Effective Hamiltonians for the Treatment of Avoided Crossings. I. Adiabatic Potential Curves. *J. Phys. B: At. Mol. Phys.* **1984**, *17*, 1235.

(15) Spiegelmann, F.; Malrieu, J. P. The Use of Effective Hamiltonians for the Treatment of Avoided Crossings. Ii. Nearly Diabatic Potential Curves. *J. Phys. B: At. Mol. Phys.* **1984**, *17*, 1259.

(16) Li, S. L.; Truhlar, D. G.; Schmidt, M. W.; Gordon, M. S. Model Space Diabatization for Quantum Photochemistry. *J. Chem. Phys.* **2015**, *142*, 064106.

(17) Pacher, T.; Cederbaum, L. S.; Köppel, H. Approximately Diabatic States from Block Diagonalization of the Electronic Hamiltonian. *J. Chem. Phys.* **1988**, *89*, 7367-7381.

(18) Cederbaum, L. S.; Schirmer, J.; Meyer, H. D. Block Diagonalisation of Hermitian Matrices. *J. Phys. A: Gen. Phys.* **1999**, *22*, 2427.

(19) Pacher, T.; Köppel, H.; Cederbaum, L. S. Quasidiabatic States from Abinitio Calculations by Block Diagonalization of the Electronic Hamiltonian: Use of Frozen Orbitals. *J. Chem. Phys.* **1991**, *95*, 6668-6680.

(20) Wu, W.; Su, P.; Shaik, S.; Hiberty, P. C. Classical Valence Bond Approach by Modern Methods. *Chem. Rev.* **2011**, *111*, 7557-7593.

(21) Grofe, A.; Qu, Z.; Truhlar, D. G.; Li, H.; Gao, J. Diabatic-at-Construction Method for Diabatic and Adiabatic Ground and Excited States Based on Multistate Density Functional Theory. *J. Chem. Theory Comput.* **2017**, *13*, 1176-1187.

(22) Song, L.; Gao, J. On the Construction of Diabatic and Adiabatic Potential Energy Surfaces Based on Ab Initio

Valence Bond Theory. *J. Phys. Chem. A* **2008**, *112*, 12925-12935.
(23) Lin, X.; Liu, X.; Ying, F.; Chen, Z.; Wu, W. Explicit Construction of Diabatic State and Its Application to the Direct Evaluation of Electronic Coupling. *J. Chem. Phys.* **2018**, *149*, 044112.
(24) Löwdin, P. O. On the Nonorthogonality Problem *Adv. Quantum Chem.* **1970**, *5*, 185-199.
(25) Löwdin, P. O. On the Non-Orthogonality Problem Connected with the Use of Atomic Wave Functions in the Theory of Molecules and Crystals. *J. Chem. Phys.* **1950**, *18*, 365-375.
(26) Araujo, M.; Lasorne, B.; Bearpark, M. J.; Robb, M. A. The Photochemistry of Formaldehyde: Internal Conversion and Molecular Dissociation in a Single Step? *J. Phys. Chem. A* **2008**, *112*, 7489-7491.
(27) Wu, W.; Song, L.; Cao, Z.; Zhang, Q.; Shaik, S. Valence Bond Configuration Interaction: A Practical Ab Initio Valence Bond Method That Incorporates Dynamic Correlation. *J Phys. Chem. A* **2002**, *106*, 2721-2726.
(28) Chen, Z. H.; Song, J. S.; Shaik, S.; Hiberty, P. C.; Wu, W. Valence Bond Perturbation Theory. A Valence Bond Method That Incorporates Perturbation Theory. **2009**, *113*, 11560-11569.
(29) Ying, F.; Su, P.; Chen, Z.; Shaik, S.; Wu, W. DFVB: A Density-Functional-Based Valence Bond Method. *J. Chem. Theory Comput.* **2012**, *8*, 1608-1615.
(30) Zhou, C.; Zhang, Y.; Gong, X.; Ying, F.; Su, P.; Wu, W. Hamiltonian Matrix Correction Based Density Functional Valence Bond Method. *J. Chem. Theory Comput.* **2017**, *13*, 627-634.
(31) Ying, F.; Zhou, C.; Zheng, P.; Luan, J.; Su, P.; Wu, W. λ-DFVB: A Valence Bond Based Multi-Configurational Density Functional Theory with a Single Variable Hybrid Parameter. *Front. Chem.* **2019**, *7*, 225.
(32) Chen, Z.; Ying, F.; Chen, X.; Song, J.; Su, P.; Song, L.; Mo, Y.; Zhang, Q.; Wu, W. XMVB 2.0: A New Version of Xiamen Valence Bond Program. *Int. J. Quan. Chem.* **2015**,*115*, 731-737.
(33) Frisch, M. J.; Trucks, G. W.; Schlegel, H. B.; Scuseria, G. E.; Robb, M. A.; Cheeseman, J. R.; Scalmani, G.; Barone, V.; Petersson, G. A.; Nakatsuji, H.*; et al. Gaussian 16 Rev. B.01*, Wallingford, CT, **2016**.
(34) MATLAB. 9.7.0.1190202 (R2019b). Natick, Massachusetts: The MathWorks Inc.; **2018**.
(35) Wilkinson, J. Householder's Method for Symmetric Matrices. *Numerische Mathematik* **1962**, *4*, 354-361.
(36) Strobach, P. The Householder Compressor Theorem and Its Application in Subspace Tracking. *Signal Processing* **2009**, *89*, 857-875.